Probabilistic seasonal outlook for the rainy season over India by monitoring the onset dates using GPM IMERG satellite-based precipitation

Jayasankar Chempampadam Balasubramannian[1,2], and Vasubandhu Misra[1,2,3]

[1]Center for Ocean-Atmospheric Prediction Studies, Florida State University, Tallahassee, Florida, USA.

[2]Department of Earth, Ocean and Atmospheric Science, Florida State University, Tallahassee, Florida, USA.

[3]Florida Climate Institute, Florida State University, Tallahassee, Florida, USA.

Corresponding Author (Jayasankar Chempampadam Balasubramannian, cbjayasankar@gmail.com)

Abstract

We utilized the Integrated Multi-Satellite Retrievals for Global Precipitation Mission version 6 (IMERG) rainfall observation (available in real time) over India to determine the onset and withdrawal of the rainy season. The annual mean climatology derived from IMERG observations over India aligned closely with the rain gauge-based India Meteorological Department observation. The IMERG rainfall time series was randomly perturbed to generate 101 ensemble members at every grid point of the rainfall analysis to obtain a corresponding ensemble of the onset and withdrawal dates of the rainy season. The perturbations were designed to sample the uncertainty due to random synoptic or mesoscale rain events influencing the diagnosis of the onset/withdrawal dates at the granularity of the IMERG observations (available at 10 km grid). Following earlier studies, we find from the IMERG dataset that seasons with an earlier onset date are strongly related to a lengthier and wetter season, whereas seasons with a later onset date correspond to a shorter and a drier season. In contrast, the connections between ENSO and IOD with the onset, withdrawal, seasonal length, and rainfall of the rainy season were comparatively weaker over most of India. The generation of ensembles in this study underscores the potential for real-time application of generating reliable, probabilistic seasonal outlooks of the rainy season over India by leveraging the local links amongst onset date, seasonal length, and seasonal rainfall anomalies. This potential is further confirmed by the high probabilistic skill scores of the seasonal outlooks using the area under the relative operating characteristic curve method.

Formatted: Swedish

Deleted: demise

Deleted: demise

Deleted: demise

Deleted: demise

Deleted: with ENSO and IOD

1. Introduction

India's water and agriculture sectors rely heavily on copious summer monsoon rainfall, emphasizing its critical role in defining the country's agrarian economy and water resource management (Gadgil and Gadgil 2006). The seasonal progression of the Indian Summer Monsoon (ISM) season has an impact not only on agricultural yields but also on other sectors such as economy and ecology (Lal 2000). Based on rainfall patterns, wind conditions, and outgoing longwave radiation, the India Meteorological Department (IMD) officially declare the date of monsoon onset over Kerala (MoK) each year. In a normal year, the ISM season begins in southern peninsular India on June 1st (with MoK), spreads throughout the country by mid-July, and then begins to retreat on September 1st (Pai et al. 2020).

There are many different definitions for the monsoon onset; however, it is typically considered as a quick, substantial, and prolonged increase in rainfall after May 10th, accompanied by a persistent change in wind direction to southwesterlies associated with the summer monsoon flow (Pai and Rajeevan 2009). In addition to the rainfall-based definitions (e.g., Ananthakrishnan and Soman 1988; Noska and Misra 2016; Misra et al. 2017b), several other atmospheric dynamical and thermodynamical variables (winds, outgoing longwave radiation, temperature, moisture flux convergence, and precipitable water) were utilized to identify the onset of summer monsoon rainfall (e.g., Fasullo and Webster 2003, Zeng and Lu 2004, Prasad and Hayashi 2005, Joseph et al. 2006, Wang et al. 2009, Walker and Bordoni 2016, Stolbova et al. 2016). These variables provide a comprehensive understanding of the atmospheric conditions and dynamics that influence the onset and total summer monsoon rainfall over India. According to Bombardi et al. (2019), monsoon onset detection methods can be grouped into local-scale and regional-to-large-scale approaches, though the latter often show weak correlation with local observations. All these approaches produce somewhat similar onset dates, but their connections with the local-scale onset of the rainfall during the ISM differ (Moron and Robertson 2014; Noska and Misra 2016; Fitzpatrick et al. 2016).

Owing to variations in the onset and withdrawal date of the monsoon season there are considerable spatial and temporal variations in the availability of the rainwater and length of the rainy season

80   (determined solely based on rain rates) over India (Joseph et al. 1994; Lal 2000; Wang et al. 2002;

81   Misra et al. 2017a; Misra et al. 2018). Preenu et al. (2017) indicate from IMD archive that the

82   earliest onset of the ISM was May 11, 1918, and the most delayed onset of ISM was Jun 18, 1972.

83   Several studies discuss the interannual variability of monsoon onset dates in India and its

84   teleconnection with El Niño and the Southern Oscillation (ENSO) and the Indian Ocean Dipole

85   (IOD, Xavier et al. 2007; Sankar et al. 2010; Misra et al. 2017a; Pradhan et al. 2017; Choudhury

86   et al. 2021). In ENSO and IOD years, the monsoon onset is altered by the modulation of the

87   teleconnections with SST anomalies in the tropical oceans, which affect the Walker and Hadley

88   circulations, respectively (Pradhan et al. 2017). Significant changes in the large-scale atmospheric

89   patterns over the monsoon areas are identified during the onset of the monsoon over India (Joseph

90   et al. 1994). According to Wang et al. (2013), the interannual variations in ocean-atmosphere

91   interaction processes significantly influence the association between the monsoon onset and

92   ENSO, which is driven by the meridional SST gradient across the Indian Ocean. Noska and Misra

93   (2016) show that the variations in the onset and withdrawal date of the rainy season over India that

94   largely overlaps with ISM are linked to the variability of the cross-equatorial upper-ocean heat

95   transport in the Indian Ocean, variations in large-scale atmospheric and oceanic circulations, and

96   regional ocean-atmosphere thermal gradients. In addition, internal variability of ISM arising from

97   intraseasonal oscillations (ISOs), can significantly influence the monsoon rainfall and as well as

98   the onset and withdrawal characteristics of the ISM (Goswami and Ajaya Mohan, 2001; Goswami

99   and Xavier, 2005; Karmakar and Misra 2019). Monsoon ISOs are typically classified into active

100 (above normal) and break (below normal) phases, and the frequency of these phases plays a crucial

101 role in determining the seasonal mean monsoon rainfall (Goswami and Ajaya Mohan, 2001).

102 Karmakar and Misra (2019) found that a majority of local onset dates (59%) occur during the

103 positive developing phases of high-frequency ISOs, while a majority of withdrawal dates (62%)

104 occur during the positive decaying phases of low-frequency ISOs.

105

106 It may be noted that we make a subtle distinction between the ISM and rainy seasons, with the

107 latter solely determined by rain rates which includes pre- and post-monsoon seasonal rainfall (e.

108 g., Noska and Misra 2016) while the former is usually a fixed calendar season (June to September)

109 and coincides additionally with the seasonal cycle of circulation features and other thermodynamic

110 factors. Figure S1 highlights the difference between the rainy season and climatological ISM (June

118 to September), which makes it evident that the rainy season accumulates more rainfall in southern

119 peninsular India and in regions east of the central monsoon region. Similarly, when compared to

120 the ISM season, the rainy season has slightly less total rainfall over both western, northern India,

121 and parts of northeastern India. It may be noted that the definition of the rainy season allows for a

122 variable length compared to the fixed calendar season of, which stems from the former including

123 pre-monsoon rainfall and rainfall from pre-monsoon and post-monsoon rainfall. For instance,

124 tropical cyclones are also included in the rainy season defined here, and they significantly

125 contribute to the annual rainfall in some parts of eastern India. Pre- and post-monsoon tropical

126 cyclones can contribute up to 25% of the yearly rainfall in some parts of India, even though the

127 southwest monsoon is the main component of our defined rainy season (Khouakhi et al. 2017).

128

129 The information about the arrival of the monsoon rainfall is imperative for farmers to plan their

130 strategy for the upcoming season. There are many attempts to predict the MoK; however, it

131 remains a challenge due to the intricate interplay between large-scale atmospheric circulation and

132 localized convective processes, resulting in substantial spatial variability in onset dates (Kung and

133 Shariff 1980; Rajeevan and Dubey 1995; Pai and Rajeevan 2007; Pradhan et al. 2017). Many

134 studies have shown that variations of the MoK have very little influence on the mean rainfall

135 anomalies of the ISM (Dhar et al. 1980; Mooley and Parthasarthy 1984; Mooley and Shukla 1987;

136 Misra and DiNapoli 2014). Furthermore, MoK is known to have insignificant relationship with

137 subsequent progression of the onset isochrones of the ISM (Bansod et al. 1991; Fasullo and

138 Webster 2003; Pai and Rajeevan 2007). Noska and Misra (2016) proposed an objective method to

139 define the onset and withdrawal of the rainy season based on area averaged all India daily rainfall,

140 and they found that mean anomalies of the rainy season are closely linked with variations in the

141 onset and withdrawal dates of the rainy season. In addition, they validated the defined onset and

142 withdrawal of the rainy season for consistency by comparing them with the seasonal evolution of

143 key dynamic and thermodynamic variables associated with the ISM. In a following study, Misra

144 et al. (2018) obtained local onset (withdrawal) dates of the Indian rainy season at the granularity

145 of the rainfall analysis and showed that they are negatively (positively) correlated with rainfall

146 anomalies of the rainy season across the Indian region. These studies suggest that monitoring the

147 local onset date of the rainy season provides a good indication of the evolution of the seasonal

148 length and rainfall of the forthcoming rainy season (i.e., the entire duration of the rainy season at

Deleted: variable

Deleted: fixed
Deleted: variable
Deleted: higher
Deleted: and
Deleted: . Notably,

Deleted: .

Deleted: But many
Deleted: seasonal

Deleted: demise
Deleted: seasonal
Deleted: demise
Deleted: .

Deleted: demise
Deleted: seasonal

Deleted: .

each grid points) and supporting its use in predictability studies. Bhardwaj and Misra (2019) found that Remotely Sensed Rainfall Products such as Tropical Rainfall Measuring Mission (TRMM) Multi-satellite Precipitation Analysis (TMPA) produce local onset and withdrawal dates similar to IMD observations. In comparison to traditionally identified onset of ISM, which are often limited to defining the onset over Kerala (e.g., MoK), the proposed method enables the generation of spatially continuous maps of onset date evolution. By capturing regional heterogeneity, it provides a more nuanced understanding of the spatiotemporal progression of onset of the rainy season across India. This simple rainfall-based definition was found useful for monitoring the onset of the rainy season in real-time and issuing the outlook of the rainy season over various regions such as Florida (Misra et al. 2022), and Central America (Rodgers et al. 2024).

Many studies have used the IMERG data set as one of their primary dataset for the analysis of the ISM (Bushair et al. 2019; Thakur et al. 2020; Saikrishna et al. 2021; Phadtare et al. 2023). In this study, we employ a rainfall-based objective method to define the local onset and withdrawal of the rainy season, leveraging the high-resolution IMERG dataset available since January 2001. Our approach captures the actual arrival and retreat of persistent rainfall at each grid point by identifying the onset and withdrawal of the rainy season. This approach also accounts for pre- and post-monsoon rainfall, providing a more complete representation of the rainy season—particularly in regions where events such as tropical cyclones contribute significantly to seasonal rainfall totals. In this study, utilizing IMERG's 12-hour latency product, we demonstrate the potential for real-time monitoring of the onset of the rainy season, which aids in anticipating the anomalies of the seasonal length and seasonal accumulated rainfall (hereafter referred to as seasonal rainfall) across India. Motivated from the grid-point level definition of onset and withdrawal dates established by Misra et al. (2018) and Bhardwaj and Misra (2019), this study advances this framework by how the IMERG 12-hour latency product can be effectively used to monitor these parameters at fine spatial scales, enabling better anticipation of anomalies of the seasonal length and seasonal rainfall. In addition, the novelty of this work lies in the use of a perturbation technique applied in the diagnosis of onset/withdrawal dates of the rainy season over India following Misra et al. (2023) and Rodgers et al. (2024) to generate 101 ensembles of daily rainfall data. This approach is the first of its kind over the Indian region and allows us to define an ensemble of local onset and withdrawal dates, aiding in the probabilistic estimate of the evolution of the rainy season that

205 accounts for observational and analysis uncertainties. Hereafter, the term 'onset' refers to local or
206 grid point-specific onset dates of the rainy season.

207

208 Additionally, this study explores the interannual variation of the evolution of the rainy season and
209 its link to large-scale forcing such as ENSO and IOD and compares their viability as predictors of
210 the rainy seasons to the local links we establish with the variations of the onset dates. We believe
211 that the insights from this study will have significant potential applications in agricultural planning
212 and water resource management.

213

214 **2. Data and Methodology**

215 **2.1 Data**

216 The analysis performed in this study utilized daily precipitation data from the IMERG version 6
217 (Huffman et al. 2019). This dataset is part of the Global Precipitation Measurement (GPM)
218 mission, which was launched in 2014 and is co-operated by NASA and the Japan Aerospace
219 Exploration Agency (JAXA). The 0.1° grid resolution (~10 km) IMERG data are available at half-
220 hourly intervals from June 2000 to the present. The dataset comprises early, late, and final run
221 products, which have latencies of approximately 4 hours (Early), 12 hours (Late), and 3.5 months
222 (Final). The IMERG late run incorporates data from multiple sources, such as satellite microwave
223 and infrared estimations, precipitation gauge analysis, and other potential precipitation estimators.
224 This dataset provides detailed temporal and spatial coverage for both the TRMM and GPM eras
225 worldwide. However, in this study, we used the daily 12-hour latency product (daily averages were
226 estimated from half-hourly products), which has great potential for monitoring the rainy season in
227 real-time. To assess the fidelity of the 12-hour latency product of IMERG over India, we have
228 compared it with the corresponding Final product of IMERG and also used rain gauge-based IMD
229 gridded rainfall data for the period 2001 - 2023 at 0.25° × 0.25° resolution (Pai et al. 2014) as a
230 validation dataset. Additionally, we defined the onset and withdrawal dates of the rainy season
231 using the daily NOAA Climate Prediction Center (CPC) precipitation data set (Xie et al. 2007)
232 and compared them with IMERG.

233

234 **2.2 Methodology**

235 **2.2.1 Onset and Retreat**

242 This study uses a simple objective definition to identify the onset and cessation dates of the wet

243 season over India which are determined by finding the minima and maxima of the cumulative

244 rainfall anomaly curve (Liebmann and Marengo 2001). The cumulative anomaly of the daily

245 rainfall at a day J (i.e., $C_i(J)$) for a year i at each grid point is estimated as:

246

247 $$C_i(J) = \sum_{j=1}^{J}(R_i(j) - R) \qquad\qquad (1)$$

248

249 where $R_i(j)$ is the rainfall for day j of year i, R is the climatology of the annual mean rainfall for a

250 given grid point. The $C_i(J)$ for 365/366 days in a year represents the cumulative rainfall anomaly

251 curve. After the onset and withdrawal dates of the season are determined, we count the number of

252 days between them to define the seasonal length. Seasonal rainfall of the rainy season refers to the

253 daily rainfall that accumulates from the day of onset date to the withdrawal date.

254

255 **2.2.2 Perturbation**

256 The motivation to perturb the timeseries is to account for the uncertainty of random synoptic or

257 mesoscale events that is potentially unrelated to the seasonal cycle, which could affect the

258 diagnosis of the onset/withdrawal date of the rainy season. The threat of false diagnosis of

259 onset/withdrawal dates of the rainy season is acute from the proposed methodology since this

260 diagnosis is computed at the granularity of the rainfall analysis. Therefore, generating an ensemble

261 of onset/withdrawal dates of the rainy season that accounts for this uncertainty is essential. The

262 perturbations are generated randomly by replacing the rainfall of each day in the original timeseries

263 for a given grid point by rainfall in the range of $\pm$ 3 days. The range of $\pm$ 3 days used in the

264 generation of the perturbed timeseries covers the uncertainty in the occurrence of the synoptic (1

265 to 7 days) to meso-scale (1 to 3 days) rain features of the rainy season. In this manner, an ensemble

266 of 101 (100 perturbations + 1 original) timeseries are generated. The diagnosis of the

267 onset/withdrawal date of the rainy season will converge or diverge amongst the ensemble members

268 if it is found to be insensitive or sensitive to these random rain events, respectively.

269

270 **2.2.3 Signal-to-noise Ratio**

271 We estimated the signal-to-noise ratio of the four quantities by utilizing the 101 ensemble

272 members.

Deleted: For a year *i*, the
Deleted: *j*
Deleted: (*j*))
Deleted: ;
Deleted: (*j*) = $\sum_{j=1}^{J}(R_i(j) - R)$
Deleted: -------------
Deleted: the
Deleted: .
Deleted: (*j*)
Deleted: demise
Deleted: estimate
Deleted: demise
Deleted: demise
Deleted: demise
Deleted: demise
Deleted: demise

289
$$S^2_{noise} = \frac{1}{A(B-1)} \sum_{a=1}^{A} \sum_{b=1}^{B} (X_{ab} - X_b)^2 \qquad (2)$$

290
$$S^2_{signal} = S^2_{em} - \frac{1}{b} S^2_{noise} \qquad (3)$$

291 Where, X belongs to any of the four quantities such as onset date, withdrawal date, seasonal length,

292 and seasonal rainfall anomalies of the varying rainy season, a and b are indices for A years and B

293 ensemble members, respectively, S^2_{em} represents the measured total signal variance in the data over

294 A years and which is defined as;

295
$$S^2_{em} = \frac{1}{(A-1)} \sum_{a=1}^{A} (X_a - \bar{X})^2 ,$$

296 And $X_a = \frac{1}{(B-1)} \sum_{b=1}^{B} X_{ab}$, $\bar{X} = \frac{1}{(A-1)} \sum_{a=1}^{A} X_a$,

297 The signal-to-noise ratio is then given by:

298
$$ratio = \frac{S^2_{signal}}{S^2_{noise}} \qquad (4)$$

299 When $ratio < 1$ then it indicates that noise (or chaotic variations) is dominant, and the signal

300 dominates when $ratio > 1$. A strong signal indicates that perturbing the rainfall time series will

301 not substantially influence the diagnostics of the onset date, withdrawal date, seasonal length, and

302 seasonal rainfall anomalies.

303

304 **2.2.4 Significance test**

305 In this study, we first estimate the two-tailed p-values of the correlation coefficients using the t-

306 statistic. Further, following Benjamini and Hochberg (1995), we conduct a test for false rejection

307 on all temporal correlations to assess its robustness, which is necessary because of the large number

308 of simultaneous statistical significance tests conducted across all grid points of the domain. This

309 process involves adjusting the p-value (Benjamini and Hochberg 1995) to control the false

310 rejection of the null hypothesis, also known as the false discovery rate. By controlling the false

311 discovery rate, we enhance the confidence in the significance of the findings.

312

313 **3. Results**

320   The seasonal mean rainfall over India observed from IMERG is found to be comparable with IMD
321   observation and superior to other satellite products over the region (Saikrishna et al., 2021). This
322   is further confirmed in Figs. 1a-c which compares the 23-year annual mean rainfall climatology
323   between IMERG observations and the corresponding IMD rainfall dataset. It may be noted that in
324   Equation (1), the annual mean rainfall climatology (R) at each grid point is used to determine
325   onset dates and withdrawal dates of the rainy season over India (e.g., Misra et al., 2018). Overall,
326   the annual mean rainfall climatology from IMERG compares well with the IMD rain gauge dataset.
327   However, the overestimation of rainfall in the Indo-Gangetic plains and parts of northeast India
328   and underestimation of rainfall over the northern Western Ghats, northern sections of northeast
329   India, and the bulk of Jammu and Kashmir by IMERG relative to IMD dataset is apparent (Fig. 1).
330   Bushair et al., (2019) noted that IMERG underestimates the rainfall over high-altitude regions
331   compared to IMD observations, which are rain gauge based. Further, Fig. 1d shows the cumulative
332   rainfall anomaly curve generated from the 23-year (2001 - 2023) daily rainfall climatology area
333   averaged over all of India for IMERG (blue) and IMD (red) observations. The onset (inflection at
334   the nadir of the cumulative anomaly curve) and withdrawal (inflection at the zenith of the
335   cumulative anomaly curve) dates estimated from IMERG and IMD closely match each other, with
336   the onset dates being 31st May and 3rd June, and the withdrawal dates being 7th October and 8th
337   October, respectively.
338

342
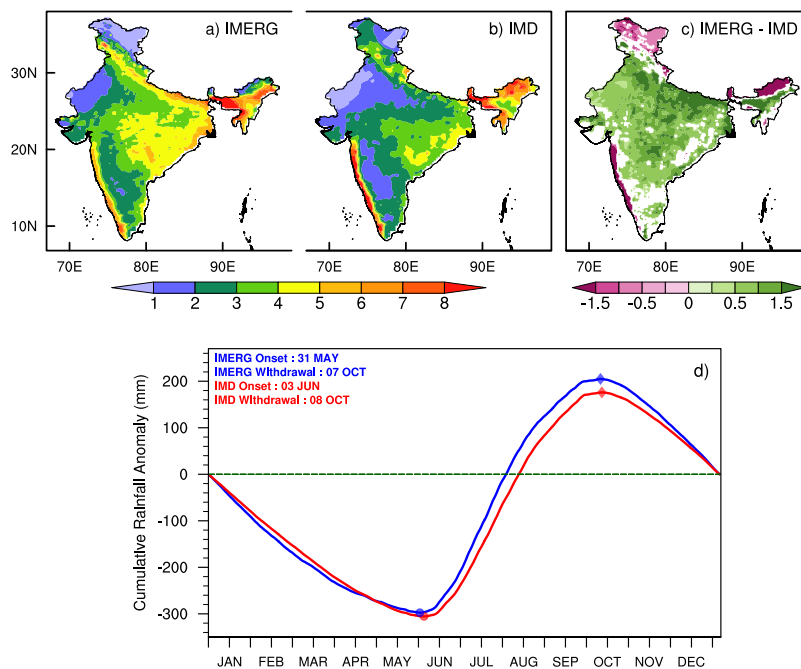
343 ***Figure 1:*** *Spatial pattern of the 23-year climatology of the mean annual rainfall (mm/day) during*

344 *the period 2001-2023 from a) IMERG observation, b) IMD observation, and c) the difference*

345 *between the IMERG and IMD (only differences significant at 5% percentile level on t-test is*

346 *shaded). d) The cumulative rainfall anomaly curve generated from the 23-year daily rainfall*

347 *climatology of IMERG (blue) and IMD (red) observations. The onset dates (filled circles) and*

348 *withdrawal dates (filled diamonds) obtained from both datasets are marked.*

349

350 Figures 2a-d depict the 23-year local climatological onset date, withdrawal date, seasonal length,

351 and seasonal accumulated rainfall from IMERG, with the associated standard deviation displayed

352 in Figs. 2e-h. The spatial distribution of the climatology of the onset dates (Fig. 2a) shows the

353 earliest onset occurs over northeast regions of India followed by southern Kerala, and then it

354 gradually advances to the other parts of the country and looks like the typical isochrone evolution

355 of the ISM (Ramage 1971; Rao 1976; Janowiak and Xie 2003). The delayed onset occurs over the

356 east coast of Tamil Nadu followed by Jammu and Kashmir. The onset dates over Kerala and
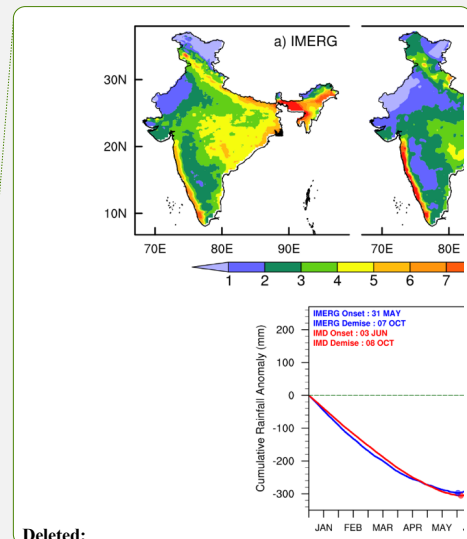
360 adjacent regions mostly start from early May and do not coincide with the MoK, and this is because

361 this methodology detects the onset dates relatively early due to strong and continuous spells of

362 pre-monsoon rainfall. Similarly, the earliest withdrawal (Fig. 2b) of the ISM occurs over

363 northwestern India such as Rajasthan, Punjab, Haryana, and Himachal Pradesh. The withdrawal

364 date is delayed over southern peninsular India, with the most delayed withdrawal occurring over

365 the southeast coast of Tamil Nadu. The seasonal length (Fig. 2c) is shorter in the west and

366 northwest regions of India, with the shortest season in Jammu and Kashmir. The longer season

367 over the peninsular India, as well as the coastal regions of Odisha and West Bengal, is linked to

368 the season's earlier start date. The spatial distribution of the seasonal accumulated rainfall (Fig.

369 2d) closely follows the typical seasonal mean ISM distribution. The standard deviation patterns of

370 the onset dates show central parts of India have less variability than other regions, such as southern

371 peninsular India, northeast, and northwest regions. Similar patterns of variability are observed in

372 the withdrawal dates and seasonal length with the largest variations found over southern peninsular

373 India and northwest India and least over central India. On the other hand, the seasonal rainfall

374 exhibits a significant range of variability across most of India, whereas comparatively less

375 variability is observed over Rajasthan and Jammu and Kashmir.
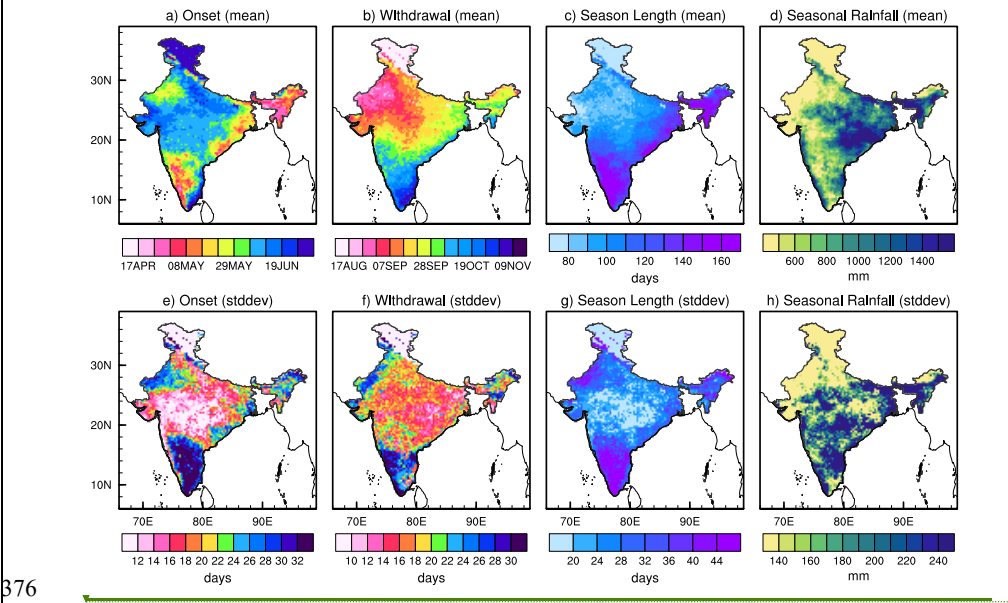
376
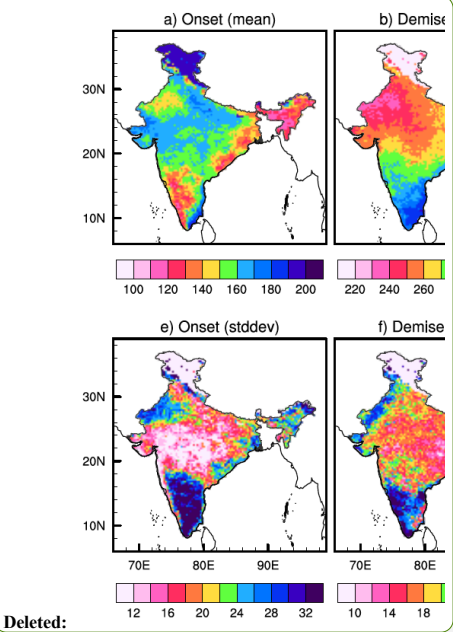
Figure 2: *The climatological a) onset date (Julian day), b) withdrawal date (Julian day), c) seasonal length, and d) seasonal accumulated rainfall (mm) of the rainy season from IMERG. The corresponding standard deviation of e) onset date (days), f) withdrawal date (days), g) seasonal length (days), and h) seasonal accumulated rainfall (mm). The contour intervals in panels (a) and (b) are at 7-day interval.*

The IMERG dataset, with its 23-year record, was compared to the IMD and CPC datasets spanning 1979–2023 (limited to this period in order for CPC and IMD to have a common period) to evaluate onset and withdrawal dates, seasonal length, and seasonal accumulated rainfall of the rainy season over India (Fig. S2). The motivation to carry out this comparison is to establish that a 23-year record of IMERG is comparable to a longer record of dataset available from the other two sources besides examining its fidelity.

It is apparent from Fig. S2 that the spatial patterns of the climatological onset and withdrawal dates, seasonal length, and rainfall in IMERG is comparable to corresponding climatologies from IMD and CPC datasets. There is however a tendency for IMERG to have a bias of a slightly earlier onset of the rainy season compared to IMD and CPC, particularly over southern peninsular India, including Kerala and Tamil Nadu (Figs. S2a-c). Similar inference can be drawn in Rajasthan, coastal Odisha and West Bengal, and few isolated grid points over other regions. In contrast, over Jammu and Kashmir, IMERG exhibits a noticeably delayed onset, which makes us unsure about the results over this area. Similarly, IMERG display a systematic bias of slightly later withdrawal dates along the Western Ghats, but overall, the rainy season withdrawal dates are consistent across datasets (Figs. S2e-g). As a result, IMERG's rainy season seems to last longer than the other two datasets in some of these locations (Figs. S2i-k). Again, in terms of seasonal accumulated rainfall (Figs. S2m-o), IMERG overestimates precipitation compared to IMD and CPC in some of these locations. However, rainfall over the Western Ghats exhibits stronger gradients and is underestimated in IMERG while it exhibits more rainfall over western central India and Tamil Nadu than the other two datasets.

The interannual variability of these variables in IMERG also appear to be comparable to the other two datasets, especially in their spatial gradients (Fig. S3). There are however instances of some

Deleted: demise

Deleted: b) demise

Deleted: c

Deleted: d

Deleted: demise

Deleted: demise

Deleted: Fig

Deleted: is observed

Deleted: costal

Deleted:

Deleted: demise

Deleted: demise

Deleted: Fig. S2d-f

Deleted: Fig. S2g-i

Deleted: Fig. S2j-l

differences in the datasets. For example, over central India, the standard deviation of seasonal rainfall is significantly overestimated in IMERG compared to IMD (Figs. S3m-o), even though the withdrawal dates (Figs. S3e-g) and seasonal length (Figs. S3i-k) exhibit less variability in IMERG.

As mentioned earlier, IMERG has few different rainfall products based on the latency of their availability in real-time. We have made comparisons of 12-hour latency product with the Final product of IMERG in Figs. S1, S2, and S3. The comparison in Fig. S1 indicates that some of the largest differences in the seasonal rain of the variable rainy season between Final and 12-hour latency of IMERG is over northern India. However, the spatial patterns of the climatological onset appear comparable (Figs. S2c and d). But the climatological withdrawal dates appear to be slightly earlier in northern India in the Final run (Fig. S2h) compared to 12-hour latency (Fig. S2g) of IMERG, which likely leads to slightly shorter length (Fig. S2l) and reduced seasonal rainfall (Fig. S2p) in the former (Fig. S2l) than in the latter (Figs. S2k and o). Some of the discrepancies observed in the 12 hour latency product of IMERG relative to IMD and CPC in Figs. S2 and S3 can likely be attributed to the uncertainty associated with the choice of the 12-hour latency product, which is an early version of IMERG with limited calibration against ground-based observations, its shorter temporal coverage of 23 years compared to the 45 years of data used for IMD and CPC. Despite these limitations, which seem to be tolerable for the applications of this study (compare Fig. 1) we are inclined to use IMERG due to its higher spatial resolution and near real-time availability making it particularly suitable for real-time applications.

The primary motivation to monitor the local onset and withdrawal of the ISM is its significant interannual variations and spatial variability (Fig. S3). Both the variation in seasonal length and seasonal rainfall are crucial in determining the nature of the rainy season (Xavier et al. 2007; Sperber and Annamalai 2014). The spatial distribution of the correlation of the local onset date with the seasonal length shows a significant negative correlation across India except in some parts of central India and Jammu and Kashmir (Fig. 3a). This negative correlation suggests that an early or later onset date is likely to be associated with a longer or a shorter rainy season, respectively. Only the correlations significant at a 5% level are shaded (non-significant values are shown in white) in Fig. 3. Similarly, early onset is associated with a wetter season, while a delayed

474 onset is linked with a drier season (Fig. 3b). However, the grid points showing significant

475 correlation are fewer in Fig. 3b compared to Fig. 3a. The correlations of the withdrawal date with

476 seasonal length (Fig. 3c) and seasonal rainfall anomalies (Fig. 3d) show that later or early

477 withdrawal of the wet season corresponds to a longer and wetter season, whereas an earlier

478 withdrawal corresponds to shorter and drier seasons. While the correlation between seasonal

479 rainfall and onset/withdrawal dates appears weaker than that with seasonal length, over 50% of

480 grid points across India still show statistically significant relationships. This is expected, as total

481 rainfall during the rainy season is influenced by variations in the seasonal length but also daily rain

482 rate, which can be influenced by various factors like tropical cyclones and intraseasonal weather

483 patterns that may lead to a weak correlation with onset/withdrawal dates. However, the withdrawal

484 date may not be a useful predictor for the rainy season because it occurs when the rainy season

485 ends. The onset and withdrawal dates are largely uncorrelated (not shown), implying that their

486 variations are independent of each other. These outcomes imply that the onset date alone can be a

487 useful predictor for the outlook of the seasonal length and the seasonal rainfall anomaly of the

488 forthcoming rainy season.

489

Deleted: demise

Deleted: demise

Deleted: demise

Deleted: demise

Deleted: Figure 3e shows that

Deleted: demise

Deleted: ,

497
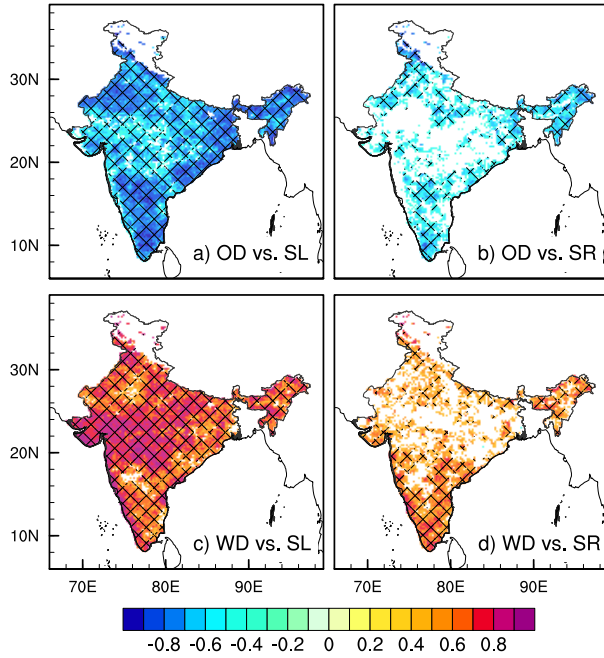
Figure 3: *The correlation coefficients of the onset date (OD) with a) seasonal length (SL), and b) seasonal rain (SR). Similarly, the correlations of withdrawal date (WD) with c) SL and d) SR. The shading indicates statistical significance at a 5% significance level according to the t-statistic (non-significant values are shown in white), following false discovery rate testing as described by Benjamini and Hochberg (1995). Cross hatchings denote correlations greater than or equal to +/- 0.6.*

We estimated the signal-to-noise ratio (Equation 4) on the four variables of onset and withdrawal dates, seasonal length, and rainfall by utilizing the 101-member ensemble of time-series data. This analysis examines the spread across ensemble members and informs on the uncertainty of the diagnosis to random rain events. The signal-to-noise ratio for onset dates (Fig. 4a) shows that noise dominates in many places, particularly in peninsular India and the eastern half of central India. These low signal-to-noise ratio regions suggests that onset dates of the rainy season are not very strongly tied to the seasonal cycle and predicting the onset dates in these places becomes challenging and less reliable. In contrast, the signal-to-noise ratios for withdrawal dates (Fig. 4b)
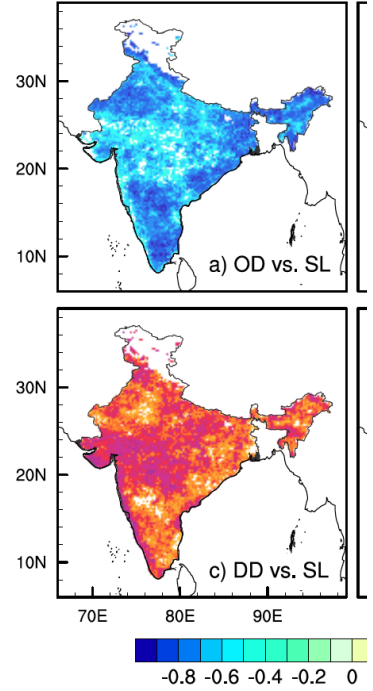
Deleted:

Deleted: *DD*

Deleted: ,

Deleted: demise

Deleted: demise

518 are typically more than one over most grid points. This indicates greater certainty for withdrawal

519 dates, particularly in areas like Kerala, coastal Karnataka, and Gujarat, where the ratios are

520 comparatively higher than one. In the case of the seasonal length, signal dominates over noise with

521 a signal-to-noise ratio above 1 over most areas (Fig. 4c). Compared to the other variables, seasonal

522 rainfall generally shows much higher signal-to-noise ratios (> 1) across most of the grid points.

523 This result is obvious given the fact that seasonal rainfall is an aggregate of the daily rainfall over

524 the entire rainy season, while the onset and withdrawal dates are single days of the season when

525 they are diagnosed. Therefore, there is a tendency for the cancellation of the noise in the

526 aggregation of the daily rainfall to seasonal rainfall, which yields a higher signal-to-noise ratio.

527
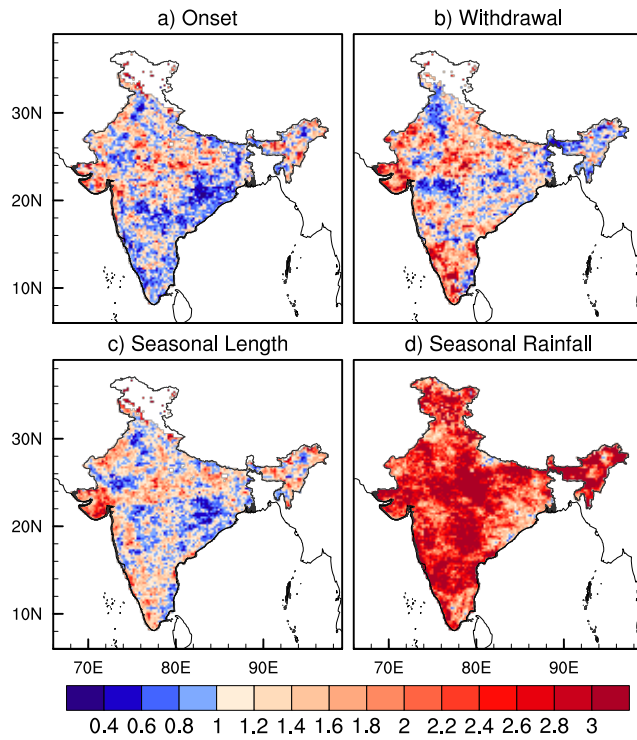
528 *Figure 4*: *The 23-year climatology of the signal-to-noise ratio of a) onset date, b) withdrawal date,*

529 *c) seasonal length, and d) seasonal rainfall estimated based on the 101 ensemble members.*
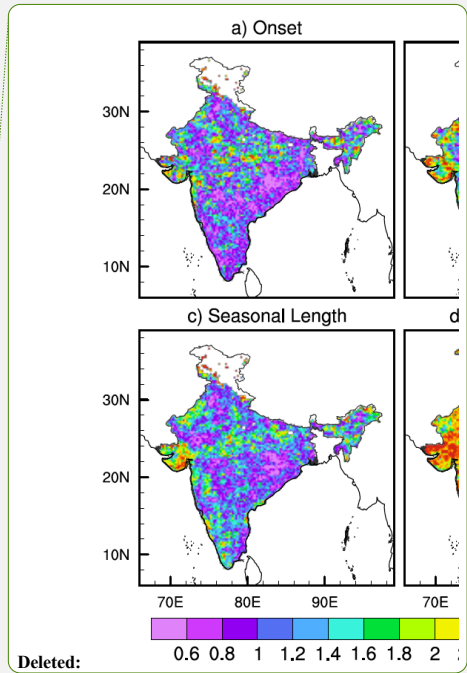
534 Further, we examined the probabilistic skill of the seasonal outlook by using the Area Under the
535 relative operating characteristic (ROC) Curve (AUC) method. The AUC method is widely used to
536 assess the skill of seasonal climate predictions (Mason and Graham 2002; Misra 2004; Narotsky
537 and Misra 2021). Previous studies have shown that this method is useful for evaluating the
538 probabilistic skill of predicting anomalous seasons based on anomalous onset dates of the rainy
539 season (e.g. Rodgers et al 2024). We categorized the onset date, seasonal length, and seasonal
540 rainfall into terciles (23-years divided into three groups): the lower tercile represents an early onset,
541 shorter season, and drier conditions; the upper tercile signifies a delayed onset, longer season, and
542 wetter conditions; and the middle tercile indicates normal onset, length, and seasonal rainfall. We
543 then created a contingency table (Table S1) to assess the probability of categorical forecasts. This
544 table evaluates how often an early or late onset is linked with a shorter or longer season and with
545 drier or wetter conditions, respectively. In addition, we also consider the effects of normal onset
546 on normal length and seasonal rainfall.
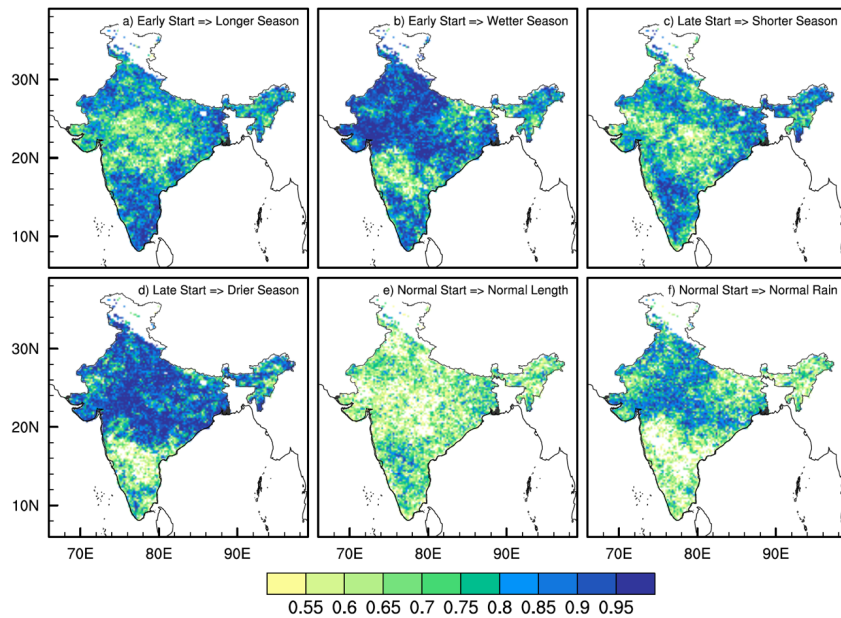
547

548 ***Figure 5****: The probabilistic skill score as measured by the Area Under the relative operating*
549 *characteristic Curve (AUC) for early start (lowest tercile) season associated with a) longer*

The probabilistic skill scores derived from the AUC method are shown in Fig. 5. Here, only grid points with AUC values ≥ 0.5 are shaded, as these points indicate skillful seasonal outlooks that outperform random predictions (Mason and Graham, 2002). The seasons with an early start and longer season (Fig. 5a) show the most skill (>0.9) over peninsular India, northwest India, and some parts of northeast India. Similarly, the early start of the season, along with the wetter season (Fig. 5b), results in high skill levels across most parts of India except the majority of Maharashtra and north interior Karnataka. The late start and associated shorter seasons shown in Fig. 5c exhibit the highest skill score over some parts of peninsular India. The late start with the drier season also resulted in high skill scores across most of the areas except Kerala, Tamil Nadu, Karnataka and Andhra Pradesh. The anomalous seasons (Fig. 5a-d) demonstrate higher skill levels across India compared to the normal seasons (Fig. 5e-f). This is due to the leveraging of the linear relationships of the onset date variations with the rainy season variations (Figs. 3a and b). In contrast, seasons with a normal start of the rainy season exhibit lower AUC skill scores (Figs. 5e and f) across most grid points relative to the anomalous start of the rainy seasons (Figs. 5a-d). However, the skill scores for a normal start with normal rainfall (Fig. 5f) are slightly better than those for a normal start with normal length (Fig. 5e). In summary, the behavior of the forthcoming season is more predictable if the onset date is early or delayed than the normal. It is easy to adopt this methodology for real-time applications. The evolution of the daily cumulative anomaly curve of rainfall could be monitored in real-time to find the minima in the curve as the onset date. However, to avoid misdiagnosing the onset date of the rainy season, one could wait for a period of time after this diagnosis (typically a week) to confirm that the minima were indeed reached to declare the onset date. Once the onset date is diagnosed then one could use the linear relationships shown in Fig. 3 to develop a seasonal outlook for the rainy season. This is done routinely in Florida (Misra et al. 2022). With the availability of the merged IMERG estimates with the rain-gauge based IMD rainfall following Mitra et al., (2009) our proposed methodology could be adopted for real-time applications over India.

581

582   Further, we investigated the interannual variability of the onset dates over India and its association

583   with ENSO (Figure S4) and the Indian Ocean Dipole (IOD) variations (Figure S5). In comparison

584   to Figure 3, Figures S4 and S5 failed the BH test suggesting the lack of robustness in the

585   teleconnections of the rainy season variations with either ENSO or IOD. It should be noted that

586   the results in Figures S4 and S4 appear to be contrary to many other studies that suggest a robust

587   teleconnection of ENSO with ISM (e. g., Webster et al. 1998, Delsole and Shukla 2002). However,

588   our variable definition of the rainy season which includes pre- and post-monsoon rainfall would

589   make the comparison with other studies dealing with fixed calendar ISM season and or all India

590   averaged rainfall of the ISM incompatible. But in light of these results that indicate a lack of strong

591   external forcing, the significance of the reliability of the seasonal outlook of the rainy season

592   shown in Figure 5 assumes greater significance. Furthermore, the monitoring of the observations

593   of the evolution of the rainy season to diagnose the onset dates seems an attractive approach with

594   the relatively low signal-to-noise ratio of the onset date of the rainy season shown in Figure 4a

595   relative to the seasonal length in Figure 4c or seasonal rainfall in Figure 4d. We are then able to

596   leverage a low signal-to-noise ratio quantity like the onset date of the rainy season to provide a

597   seasonal outlook of relatively higher signal-to-noise ratio quantities of seasonal length and rainfall.

598

599   **4. Summary and Concluding Remarks**

600   The seasonal prediction of the Indian rainy season is a considerable challenge given its complex

601   spatio-temporal variations. In this study, we offer a simple and reliable technique for seasonal

602   outlook of the rainy season, which is viable for real-time applications as well. Using precipitation

603   estimates of IMERG version 6 over India at 10km grid, we generate an ensemble of 101 members

604   from randomly perturbing the series to assess the uncertainty of the diagnosed onset/withdrawal

605   dates of the rainy season to random synoptic-meso scale rain events unconnected to the seasonal

606   cycle. The proposed method generates a spatial distribution of local-scale onset and withdrawal

607   dates, capturing regional variations and offering a nuanced view of progression rainy season across

608   India. Such location-specific information is useful for practical applications such as agriculture,

609   disaster planning, and water management.

610

Deleted: In light of these results, the significance of the reliability of the seasonal outlook

Deleted: lower

Deleted: demise

615 We verified the IMERG rainfall observations against gauge-based IMD observations. The mean
616 annual rainfall climatology of IMERG closely matches that of the IMD. However, IMERG tends
617 to underestimate mean annual rainfall in high-altitude regions and overestimate it in the Indo-
618 Gangetic plains. Further, we examined the relationships between the onset and withdrawal dates
619 with seasonal length and rainfall and discovered that variations in onset and withdrawal dates of
620 the rainy season across India have a significant impact on the seasonal length and the seasonal
621 rainfall variations of the rainy season. It is found that an earlier onset date of the rainy season is
622 strongly related to a longer and wetter season, whereas a later onset date corresponds to a shorter
623 and drier season. However, the relationship between the onset, withdrawal, seasonal length, and
624 rainfall with large-scale climate drivers such as ENSO and IOD is comparatively weaker in major
625 parts of India. Although the influence of ENSO and IOD were investigated in this study, future
626 research could investigate the influence of additional teleconnection patterns such as the Madden–
627 Julian Oscillation (MJO), Pacific Decadal Oscillation (PDO), and North Atlantic Oscillation
628 (NAO), which may also modulate the timing and characteristics of the rainy season.
629
630 This study shows that by estimating the onset date of the rainy season alone we can effectively
631 provide a reliable seasonal outlook for both the seasonal length and total rainfall of the upcoming
632 season by exploiting the existing local relationships. The low signal to noise ratio of the onset date
633 of the rainy season suggests the dominance of internal variations, which will be a challenge for its
634 seasonal predictability. However, by way of monitoring the evolution of the onset date we can
635 leverage its local relationship with the length and seasonal rainfall anomaly to provide reliable
636 seasonal outlook of the rainy season. The probabilistic skill scores of these seasonal outlooks
637 generated from the monitoring of the onset date variations present an objective measure of its high
638 confidence of reliability. Compared to traditional ISM onset definitions, which often focus on
639 Kerala (e.g., MoK), the proposed method can generate spatial maps of local-scale onset dates of
640 the rainy season. It captures regional heterogeneity and the progression of the rainy season across
641 India. Since the method is based on the rainy season and includes pre- and post-monsoon rainfall,
642 it provides a comprehensive viewpoint of the rainy season. These seasonal outlooks have
643 numerous potential applications, and many local communities could greatly benefit from them.
644 The proposed methodology for the seasonal outlook of the rainy season over India demonstrates

Deleted: demise

Deleted: demise

Deleted: demise

Formatted: Font color: Auto

Deleted: The probabilistic skill scores presented in this study also demonstrate that this method has a high potential for providing seasonal outlooks for the forthcoming season.

Deleted: could be easily adapted

its adaptation for real-time applications from the current availability of IMERG rainfall products in real-time.

Acknowledgments

We acknowledge the support from NASA grant 80NSSC22K0595.

Code/Data Availability

The IMERG rainfall dataset is available from the NASA GES DISC (https://gpm1.gesdisc.eosdis.nasa.gov/data/GPM_L3/GPM_3IMERGDL.06/). The India Meteorological Department rainfall data set used for the analysis in this study is available at https://www.imdpune.gov.in/cmpg/Griddata/Rainfall_25_NetCDF.html. The daily CPC data is obtained from https://psl.noaa.gov/data/gridded/data.cpc.globalprecip.html. The Python and NCL codes used for the analysis can be provided by the corresponding authors upon request.

Author contribution

The study was conceptualized by CBJ and VM. CBJ carried out the analysis and validation and prepared the original manuscript. VM supervised the work, acquired funding, and reviewed and edited the manuscript.

Competing interests

The authors declare that they have no conflict of interest.

Reference:

1. Ananthakrishnan, R., and M. K. Soman, (1988). The onset of the southwest monsoon over Kerala: 1901–1980. J. Climatol., **8**, 283–296, doi:10.1002/joc.3370080305.
2. Bansod, S. D., S. V. Singh, and R. H. Kripalani, 1991: The relationship of monsoon onset with subsequent rainfall over India. *Int. J. Climatol.*, **11**, 809–817, doi:10.1002/joc.3370110707.
3. Benjamini, Y., & Hochberg, Y. (1995). Controlling the false discovery rate: A practical and powerful approach to multiple testing. Journal of the Royal Statistical Society: Series B, 57(1), 289–300. https://doi.org/10.1111/j.2517-6161.1995.tb02031.x

685   4. Bhardwaj, A., & Misra, V. (2019). Monitoring the Indian summer monsoon evolution at
686   the granularity of the Indian meteorological sub-divisions using remotely sensed rainfall
687   products. Remote Sensing, 11(9), 1080. https://doi.org/10.3390/rs11091080

688   5. Bombardi, R. J., Moron, V., & Goodnight, J. S. (2020). Detection, variability, and
689   predictability of monsoon onset and withdrawal dates: A review. Int. J. Climatol, 40(2),
690   641-667. https://doi.org/10.1002/joc.6264

691   6. Bushair, M. T., Kumar, P., & Gairola, R. M. (2019). Evaluation and assimilation of various
692   satellite-derived rainfall products over India. International Journal of Remote Sensing, 1–
693   24. https://doi.org/10.1080/01431161.2019.1579389

694   7. Choudhury, D., Nath, D., & Chen, W. (2021). The modulation of Indian summer monsoon
695   onset processes during ENSO through equatorward migration of the subtropical jet
696   stream. Climate Dynamics, 57(1), 141-152. https://doi.org/10.1007/s00382-021-05700-4.

697   8. Delsole, T, and J. Shukla, (2002). Linear prediction of Indian Monsoon Rainfall. J. Climate,
698   15, 3645-3658. https://doi.org/10.1175/1520-0442(2002)015<3645;LPOIMR>2.0.CO;2

699   9. Dhar, O. N., P. R. Rakhecha, and B. N. Mandal (1980), Does the early or late onset of
700   monsoon provide any clue to subsequent rainfall during the monsoon season, Mon.
701   Weather Rev., 108, 1069–1072, doi:10.1175/1520-0493(1980)1082.0.CO;2

702   10. Fasullo J, Webster PJ (2003) A hydrological definition of Indian monsoon onset and
703   withdrawal. J Climate 16:3200–321. https://doi.org/10.1175/1520-
704   0442(2003)016<3200a:AHDOIM>2.0.CO;2

705   11. Fitzpatrick, R. G., Parker, D. J., & Willetts, P. D. (2016). Assessing the level of spatial
706   homogeneity of the agronomic Indian monsoon onset. Geophysical Research Letters,
707   43(22), 11-867. https://doi.org/10.1002/2016GL070711

708   12. Gadgil, S.; Gadgil, S. (2006). The Indian Monsoon, GDP and Agriculture. Econ. Polit.
709   Wkly. 41, 4887–4895. https://www.jstor.org/stable/4418949

710   13. Goswami, B. N., & Mohan, R. A. (2001). Intraseasonal oscillations and interannual
711   variability of the Indian summer monsoon. Journal of climate, 14(6), 1180-1198.
712   https://doi.org/10.1175/1520-0442(2001)014<1180:IOAIVO>2.0.CO;2

713   14. Goswami, B. N., & Xavier, P. K. (2005). ENSO control on the south Asian monsoon
714   through the length of the rainy season. Geophysical Research Letters, 32(18).
715   https://doi.org/10.1029/2005GL023216

Moved (insertion) [1]

Deleted: 3211

Deleted: .

Deleted: 2006,

15. Huffman, G. J., Bolvin, D. T., Braithwaite, D., Hsu, K. L., Joyce, R. J., Kidd, C., ... & Xie, P. (2020). Integrated multi-satellite retrievals for the global precipitation measurement (GPM) mission (IMERG). In *Satellite precipitation measurement: Volume 1* (pp. 343-353). Cham: Springer International Publishing. https://doi.org/10.1007/978-3-030-24568-9_19

16. Janowiak, J. E., and P. Xie (2003), A global-scale examination of monsoon-related precipitation, J. Clim., 16, 4121–4133. https://doi.org/10.1175/1520-0442(2003)016<4121:AGEOMP>2.0.CO;2

17. Joseph PV, Eishcheid JK, Pyle RJ. (1994). Interannual variability of the onset of the Indian summer monsoon and its association with atmospheric features, El Nino, and sea surface temperature anomalies. Journal of Climate 7: 81–105. https://doi.org/10.1175/1520-0442(1994)007<0081:IVOTOO>2.0.CO;2

18. Joseph PV, Sooraj KP, Rajan CK (2006). The summer monsoon onset process over South Asia and an objective method for the date of monsoon onset over Kerala. Int J Climatol 26:1871–1893. https://doi.org/10.1002/joc.1340

19. Karmakar, N., & Misra, V. (2019). The relation of intraseasonal variations with local onset and demise of the Indian summer monsoon. *Journal of Geophysical Research: Atmospheres*, *124*(5), 2483-2506. https://doi.org/10.1029/2018JD029642

20. Khouakhi, A., Villarini, G., & Vecchi, G. A. (2017). Contribution of tropical cyclones to rainfall at the global scale. Journal of Climate, 30(1), 359-372. https://doi.org/10.1175/JCLI-D-16-0298.1

21. Kung, E. C., and Sharif, T. A., (1980). Regression forecasting of the onset of the India summer monsoon with antecedent upper air conditions, J. Appl. Meteorol., V19, pp370—380. https://doi.org/10.1175/1520-0450(1980)019<0370:RFOTOO>2.0.CO;2

22. Lal, M. (2000). Climatic change-implications for India's water resources. Journal of Social and Economic Development, 3, 57-87. https://ideas.repec.org/a/sch/journl/v3y2001i1p57-87.html

23. Liebmann, B., and J. Marengo, (2001). Interannual variability of the rainy season and rainfall in the Brazilian Amazon basin. J. Climate, 14, 4308–4318, https://doi.org/10.1175/1520-457 0442(2001) 014,4308:IVOTRS.2.0.CO;2.

24. Mason, S. J. and N. E. Graham, (2002). Areas beneath the relative operating characteristics (ROC) and relative operating levels (ROL) curves: statistical significance and

interpretation. Quar. Roy. Soc., 128, 2145-2166. https://doi.org/10.1256/003590002320603584

25. Misra, V. (2004) An evaluation of the predictability of austral summer season precipitation over South America. Journal of Climate, **17**, 1161–1175. https://doi.org/10.1175/1520-0442(2004)017<1161:AEOTPO>2.0.CO;2

26. Misra, V., Dixit, S., & Jayasankar, C. B. (2023). The regional diagnosis of onset and demise of the rainy season over tropical and subtropical Australia. Earth Interactions, 27(1), 220026. https://doi.org/10.1175/EI-D-22-0026.1

27. Misra, V., Jayasankar, C. B., Beasley, P., & Bhardwaj, A. (2022). Operational monitoring of the evolution of rainy season over florida. Frontiers in Climate, 4, 793959. https://doi.org/10.3389/fclim.2022.793959

28. Misra, V.; Bhardwaj, A.; Mishra, A. (2018). Local onset and demise of the Indian summer monsoon. Clim. Dyn., 51, 1609–1622. https://doi.org/10.1007/s00382-017-3924-2

29. Misra, V.; Bhardwaj, A.; Noska, R. (2017) Understanding the Variations of the Length and the Seasonal Rainfall Anomalies of the Indian Summer Monsoon. J. Clim., 30, 1753–1763. https://doi.org/10.1175/JCLI-D-16-0501.1

30. Misra V, DiNapoli S (2014) The variability of the southeast Asian summer monsoon. Int J Climatol 34:893–901. https://doi.org/10.1002/joc.3735

31. Mitra, A. K., Bohra, A. K., Rajeevan, M. N., & Krishnamurti, T. N. (2009). Daily Indian precipitation analysis formed from a merge of rain-gauge data with the TRMM TMPA satellite-derived rainfall estimates. 87A, 265-279. https://doi.org/10.2151/jmsj.87A.265

32. Mooley, D. A., and B. Parthasarthy (1984), Fluctuations in all-India summer monsoon rainfall during 1871–1978, Clim. Change, 6(3), 287–301, doi:10.1007/BF00142477. https://doi.org/10.1007/BF00142477

33. Mooley, D. A., and J. Shukla (1987), Variability and forecasting of the summer monsoon rainfall over India, in Monsoon Meteorology, edited by C. P. Chang and T. N. Krishnamurti, pp. 26–59, Oxford Univ. Press, Oxford, U. K

34. Moron V, Robertson AW, (2014): Interannual variability of Indian summer monsoon rainfall onset date at local scale. Int J Climatol, 34(4). doi:10.1002/joc.3745

35. Noska, R.; Misra, V. (2016) Characterizing the onset and demise of the Indian summer monsoon. Geophys. Res. Lett., 43, 4547–4554. https://doi.org/10.1002/2016GL068409

799   36. Pai DS, Rajeevan M (2007) Indian Summer Monsoon Onset: variability and prediction.
800   NCC Research Report No. 6. National Climate Centre, Indian Meteorological Department.
801   37. Pai, D. S., & Rajeevan, M. N. (2009). Summer monsoon onset over Kerala: New definition
802   and prediction. Journal of Earth System Science, 118(2), 123-135.
803   https://doi.org/10.1007/s12040-009-0020-y
804   38. Pai, D. S., Rajeevan, M., Sreejith, O. P., Mukhopadhyay, B., & Satbha, N. S. (2014).
805   Development of a new high spatial resolution (0.25× 0.25) long period (1901-2010) daily
806   gridded rainfall data set over India and its comparison with existing data sets over the
807   region. Mausam, 65(1), 1-18. https://doi.org/10.54302/mausam.v65i1.851
808   39. Pai, D. S., Bandgar Arti, Devi Sunitha, Musale Madhuri, M. R. Badwaik, A. P. Kundale,
809   Gadgil Sulochana, M. Mohapatra, and M. Rajeevan. (2020) "Normal dates of
810   onset/progress and withdrawal of southwest monsoon over India." Mausam 71, no. 4, 553-
811   570. https://doi.org/10.54302/mausam.v71i4.33
812   40. Phadtare, J. A., Fletcher, J. K., Ross, A. N., Turner, A. G., Schiemann, R. K., & Burns, H.
813   L. (2023). Unravelling the mechanism of summer monsoon rainfall modes over the west
814   coast of India using model simulations. Quarterly Journal of the Royal Meteorological
815   Society, 149(757), 3164-3182. https://doi.org/10.1002/qj.4550
816   41. Pradhan, M., Rao, A. S., Srivastava, A., Dakate, A., Salunke, K., & Shameera, K. S. (2017).
817   Prediction of Indian summer-monsoon onset variability: A season in advance. Scientific
818   reports, 7(1), 14229. https://doi.org/10.1038/s41598-017-12594-y
819   42. Prasad, V. S. & Hayashi, T. Onset and withdrawal of Indian summer monsoon. Geophys.
820   Res. Lett. 32, 1–5 (2005). https://doi.org/10.1029/2005GL023269
821   43. Preenu, P. N., Joseph, P. V., & Dineshkumar, P. K. (2017). Variability of the date of
822   monsoon onset over Kerala (India) of the period 1870–2014 and its relation to sea surface
823   temperature. Journal of Earth System Science, 126, 1-19. https://doi.org/10.1007/s12040-
824   017-0852-9
825   44. Rajeevan, M. and Dubey, D. P., (1995) Long range prediction of monsoon onset over
826   Kerala, Mausam, V46, pp287-290. https://doi.org/10.54302/mausam.v46i3.3261
827   45. Ramage, C. (1971), Monsoon Meteorology, Int. Geophys. Ser., vol. 15, 296 pp., Academic
828   Press, San Diego, Calif.

Deleted:

Deleted: (2020):

Formatted: Dutch

Deleted: ,

46. Ramesh Kumar, M. R., (2004) Forecasting of onset of southwest monsoon over Kerala coast using satellite data, IEEE Geosci. Remote Sens. Lett., V1 (4), pp265-267. 10.1109/LGRS.2004.832226

47. Rao, Y. P. (1976) Southwest monsoon. Meteorological Monograph, Synoptic Meteorology, 367.

48. Rodgers, J., Misra, V., & Jayasankar, C. B. (2024). Using the observed variations of the start date of the rainy season over Central America for its reliable seasonal outlook. Journal of Climate. 37(18), 4901–4913. https://doi.org/10.1175/JCLI-D-23-0699.1

49. Saikrishna, T. S., Ramu, D. A., & Osuri, K. K. (2021). Inter-comparison of high-resolution satellite precipitation products over India during the summer monsoon season. Meteorology and Atmospheric Physics, 133, 1675-1690. https://doi.org/10.1007/s00703-021-00829-7

50. Sankar, S., Kumar, M. R., & Reason, C. (2011). On the relative roles of El Nino and Indian Ocean Dipole events on the Monsoon Onset over Kerala. Theoretical and applied climatology, 103, 359-374. https://doi.org/10.1007/s00704-010-0306-7

51. Sperber, K. R., and H. Annamalai, (2014) The use of fractional accumulated precipitation for the evaluation of the annual cycle of monsoons. Climate Dyn., 43, 3219–3244, doi:10.1007/s00382-014-2099-3.

52. Stolbova, V., Surovyatkina, E., Bookhagen, B., & Kurths, J. (2016). Tipping elements of the Indian monsoon: Prediction of onset and withdrawal. Geophysical Research Letters, 43(8), 3982-3990. https://doi.org/10.1002/2016GL068392

53. Thakur, M. K., Kumar, T. L., Narayanan, M. S., Kundeti, K. R., & Barbosa, H. (2020). Analytical study of the performance of the IMERG over the Indian landmass. Meteorological Applications, 27(3), e1908. https://doi.org/10.1002/met.1908

54. Walker, J. M., & Bordoni, S. (2016). Onset and withdrawal of the large-scale South Asian monsoon: A dynamical definition using change point detection. Geophysical Research Letters, 43(22), 11-815. https://doi.org/10.1002/2016GL071026

55. Wang B, Ding Q, Joseph PV (2009) Objective definition of the Indian summer monsoon onset. J Clim 22(12):3303–3316. https://doi.org/10.1175/2008JCLI2675.1

56. Wang B, LinHo (2002) Rainy season of the Asia-Pacific summer monsoon. J Climate 15:386–398. https://doi.org/10.1175/1520-0442(2002)015<0386:RSOTAP>2.0.CO;2

57. Wang, X., Jiang, X., Yang, S., & Li, Y. (2013). Different impacts of the two types of El Niño on Asian summer monsoon onset. Environmental Research Letters, 8(4), 575–591. DOI 10.1088/1748-9326/8/4/044053

58. Webster, P.   J., V.   O. Magana, T.   N. Palmer, J. Shukla, R.   A. Tomas, M. Yanai, and T. Yasunari, (1998) Monsoons: Processes, predictability, and the prospects for prediction. *J. Geophys. Res., **103**,* 14451–14510. https://doi.org/10.1029/97JC02719

59. Xavier, P. K., C. Marzin, and B. N. Goswami, 2007: An objective definition of the Indian summer monsoon season and a new perspective on the ENSO–monsoon relationship. Quart. J. Roy. Meteor. Soc., 133, 749–764, doi:10.1002/qj.45.

60. Xie, P., A. Yatagai, M. Chen, T. Hayasaka, Y. Fukushima, C. Liu, and S. Yang (2007), A gauge-based analysis of daily precipitation over East Asia, J. Hydrometeorol., 8, 607. 626. https://doi.org/10.1175/JHM583.1

61. Zeng X, Lu E (2004) Globally unified monsoon onset and retreat indexes. J Climate 17:2241–2248. https://doi.org/10.1175/1520-0442(2004)017<2241:GUMOAR>2.0.CO;2